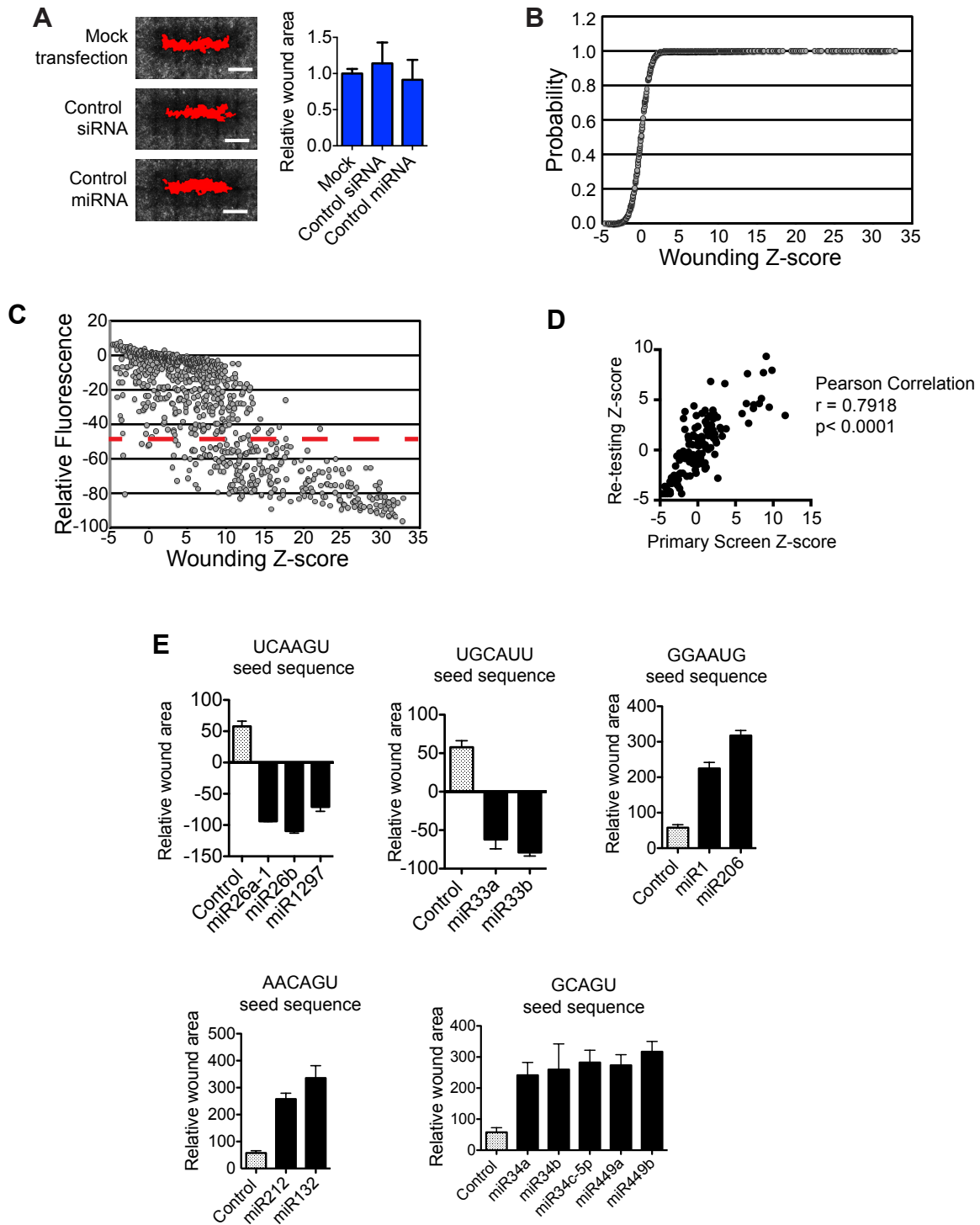


Supplementary Figure S1, Dang et. al.

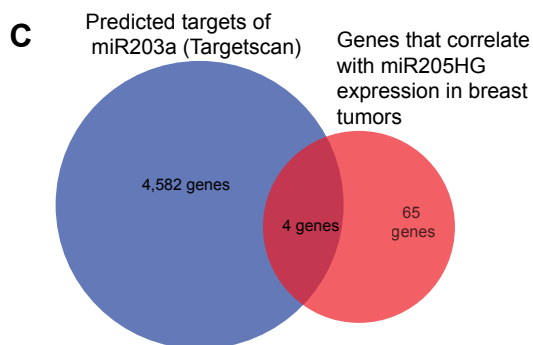
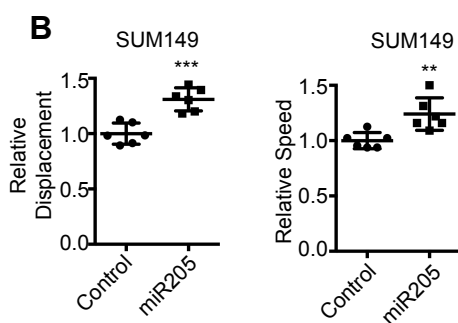


Supplementary Figure S1. Regulation of motility by miRNAs. (A) Wound healing of phalloidin stained MCFDCIS cells. “Mock transfected” cells were treated with RNAiMAX, but no siRNA or miRNA. “Control siRNA” cells were transfected with a siRNA pool that does not target human genes. “Control miRNA” cells were transfected with miR545, which does not induce a detectable phenotype. Graph shows the relative wound area (mean + standard deviation (SD), n= 9 wounds from 3 independent experiments). No significant difference between the means of each condition were detected by Student’s t-test. (B) Cumulative distribution plot of the wound healing z-scores calculated for individual miRNA mimics in the screen. (C) Graph of the relative fluorescence activity (y) and wound healing z-scores (x) of individual miRNAs. Relative fluorescence was determined by measuring the signal intensity from Hoechst staining of the same wells evaluated for the wound assay in the screen. (D) Graph showing the wound healing z-scores from the re-testing of 132 mimics (y) compared to their z-scores from the primary screen (x). (E) Graphs show the normalized wound activity scores from the primary screen for the indicated seed sequences corresponding to at least 2 distinct miRNA mimics. Negative activity scores indicate more complete wound closure compared to control.

Supplementary Figure S2, Dang et. al.

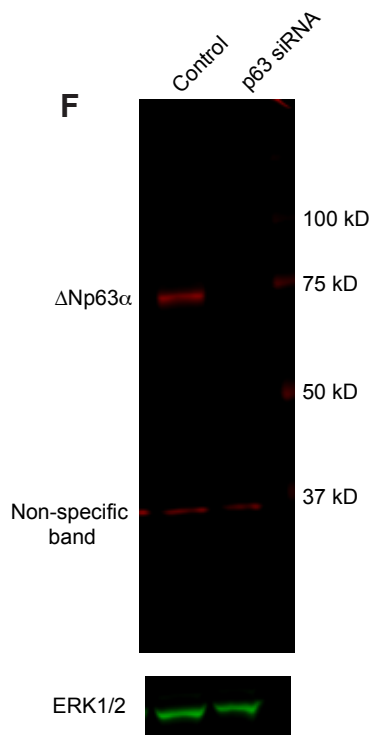
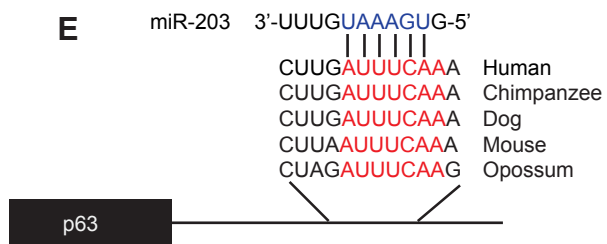
A

Cell line	Estrogen Receptor	HER2	Subtype	Migratory phenotype
MCFDCIS	Negative	Negative	Basal-like	Motile
HCC1806	Negative	Negative	Basal-like	Motile
HCC1954	Negative	Positive	Basal-like	Motile
HCC1428	Positive	Negative	Luminal-type	Non-motile
T47D	Positive	Negative	Luminal-type	Non-motile
MCF7	Positive	Negative	Luminal-type	Non-motile



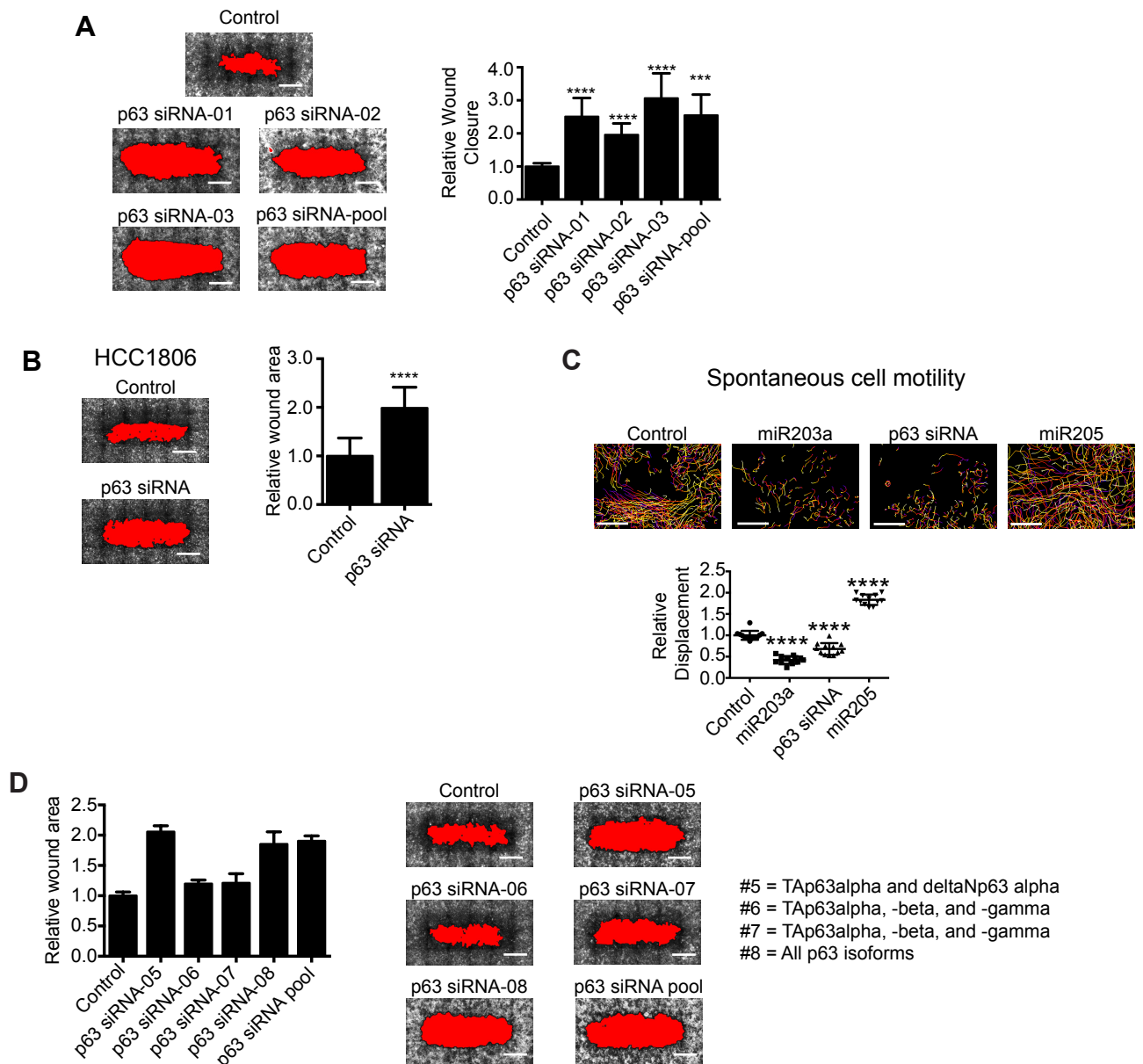
D Correlation with miR-205HG expression in breast tumors

Gene Symbol	Pearson Score	Spearman Score
TP63	0.49	0.52
COL17A1	0.4	0.47
CLCA4	0.35	0.4
KIAA1456	0.3	0.37



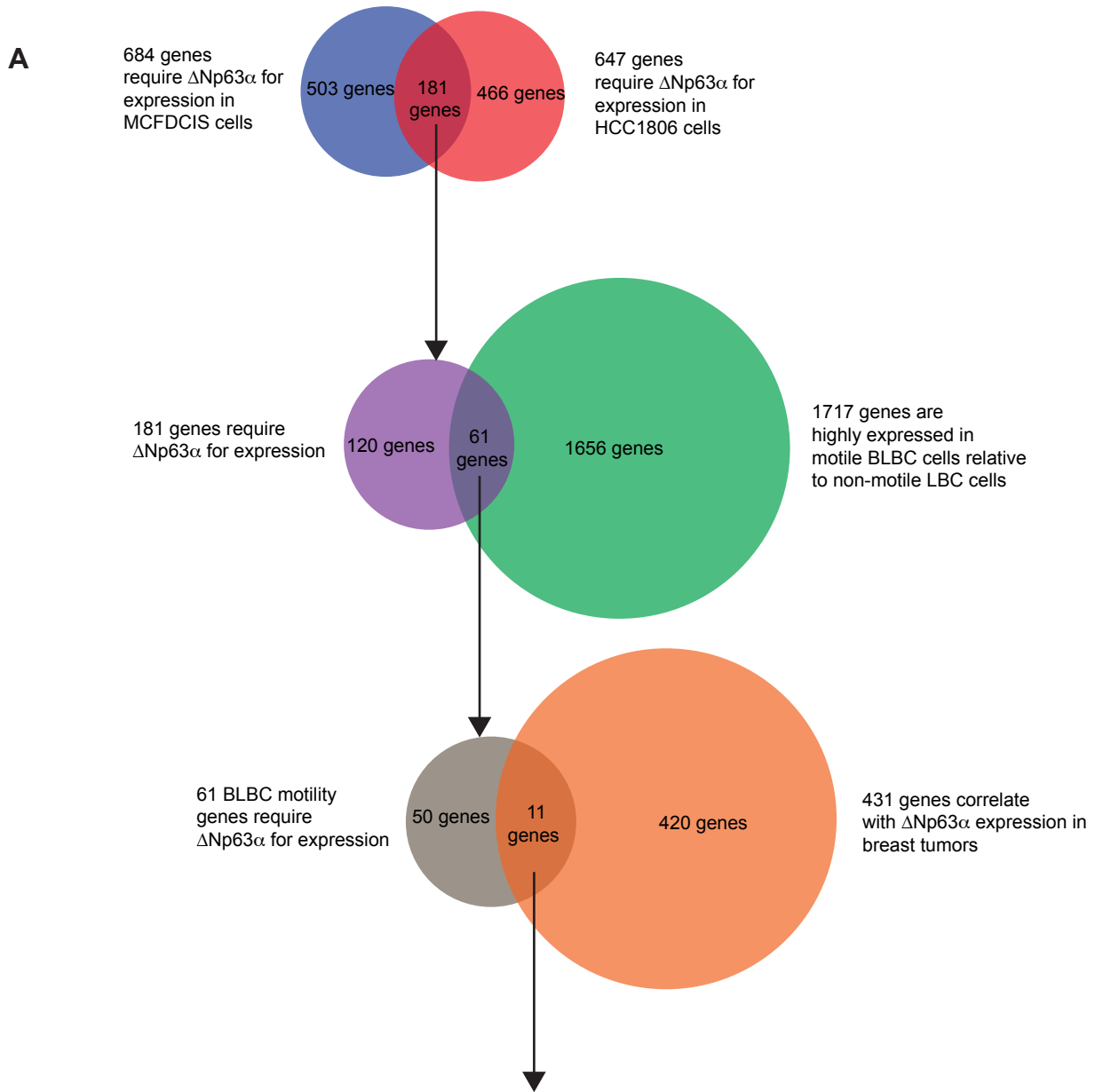
Supplementary Figure S2. Cell signaling pathways silenced by miR203a. (A) Summary of molecular and phenotypic characteristics of basal-like and luminal-type breast cancer cell lines. (B) Subconfluent SUM149 cells transfected indicated and imaged for 7 h. Graphs show speed and displacement (mean \pm SD, n=12 x,y positions over 2 experiments). **p < 0.01, ***, p < 0.001, unpaired Student's t-test. (C) Venn diagram showing the overlap in predicted miR203a targets and genes that are co-expressed with the miR205 host gene (miR205HG) in breast tumors (Spearman and Pearson correlation \geq 0.3). (D) List of the 4 genes that are predicted targets of miR203a and co-expressed with miR205HG. TP63= p63. (E) Graphic showing the predicted miR203a target sequence in the 3' UTR of the p63 gene in the indicated species. Target predication was determined using Targetscan. (F) Immunoblot of MDCDCIS cells transfected as indicated. An antibody that detects all 6 p63 isoforms was used. ERK1/2 expression in the same gel lanes serves as a loading control. (G) Immunoblot showing the expression of Δ Np63 α in MCFDCIS and MCFDCIS- Δ Np63 α cells.

Supplementary Figure S3, Dang et. al.



Supplementary Figure S3. Regulation of cell motility by Δ Np63 α . (A) Wound healing of MCFDCIS cells transfected with control or p63 siRNAs. Scale bars, 1 mm. Graphs show quantification of relative wound area (mean + SD, n=6 wounds from 2 independent experiments). ***, $p < 0.001$, **** $p < 0.0001$, unpaired Student's test. (B) Wound healing of HCC1806 cells transfected with control or p63 siRNAs. Scale bars, 1 mm. Graph shows relative wound area (mean + SD, n=6 wounds from 2 independent experiments). **** $p < 0.0001$, unpaired Student's test. (C) Subconfluent MCFDCIS cells were transfected and imaged for 7 h. Scale bars, 100 μ m. Graphs show displacement (mean + SD, n= 12 x,y positions over 2 experiments). **** $p < 0.0001$, unpaired Student's test. (D) Wound healing of MCFDCIS cells transfected with control or p63 siRNAs that are distinct from the p63 siRNAs shown in (A). The p63 isoforms targeted by the siRNAs is indicated on the right. Only siRNAs that silence can Δ Np63 α reduced the rate of wound closure. Scale bars, 1 mm. Graph show quantification of relative wound area (mean + SD, n=6 wounds from 2 independent experiments).

Supplementary Figure S4, Dang et. al.



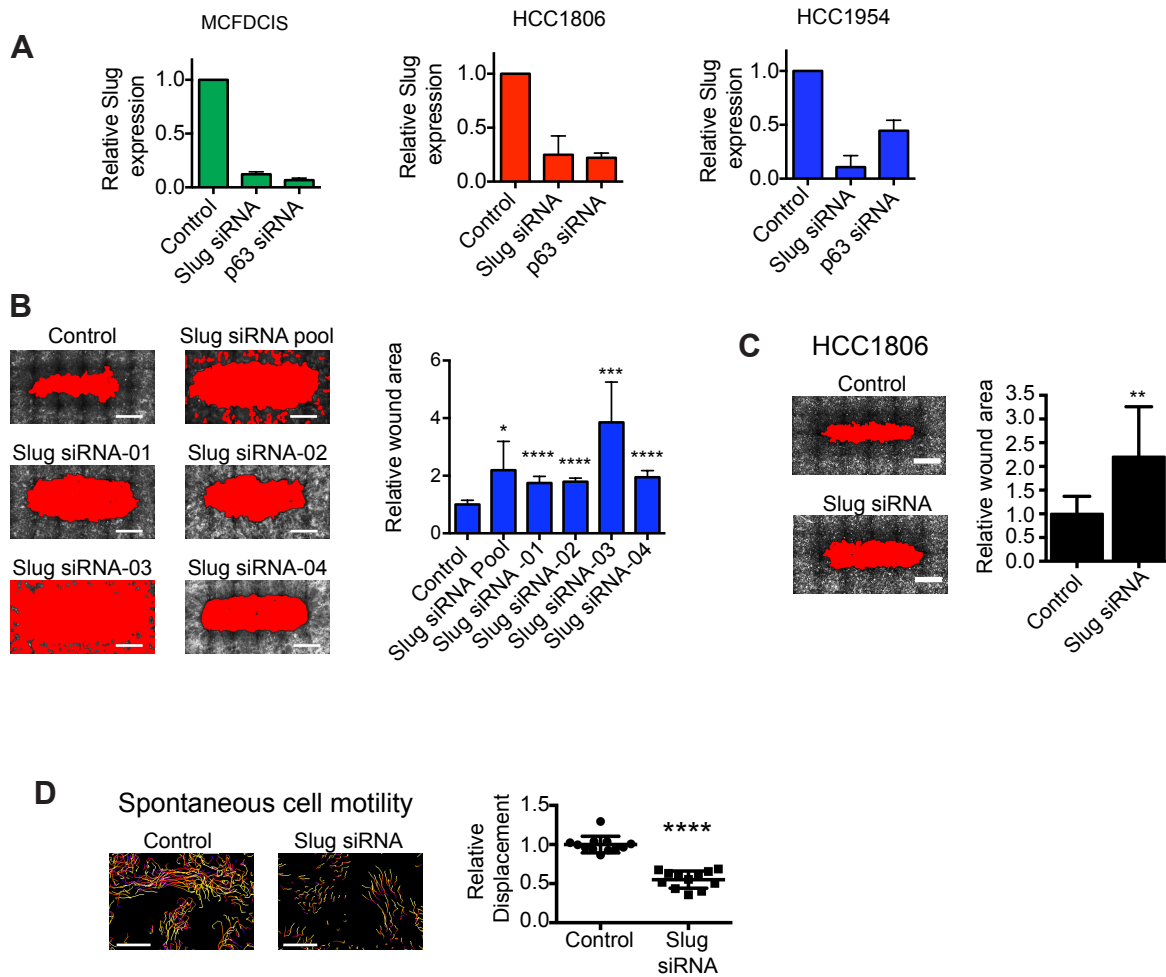
B

Correlation with p63 expression in breast tumors

Gene Symbol	Pearson Score	Spearman Score
FAT2	0.61	0.62
DST	0.59	0.62
ANXA8L1	0.57	0.63
MAMDC2	0.54	0.54
DLK2	0.41	0.37
SNAI2	0.37	0.37
PALMD	0.37	0.36
PTPRZ1	0.36	0.47
VSNL1	0.34	0.37
GNG11	0.31	0.33
SNCA	0.31	0.31

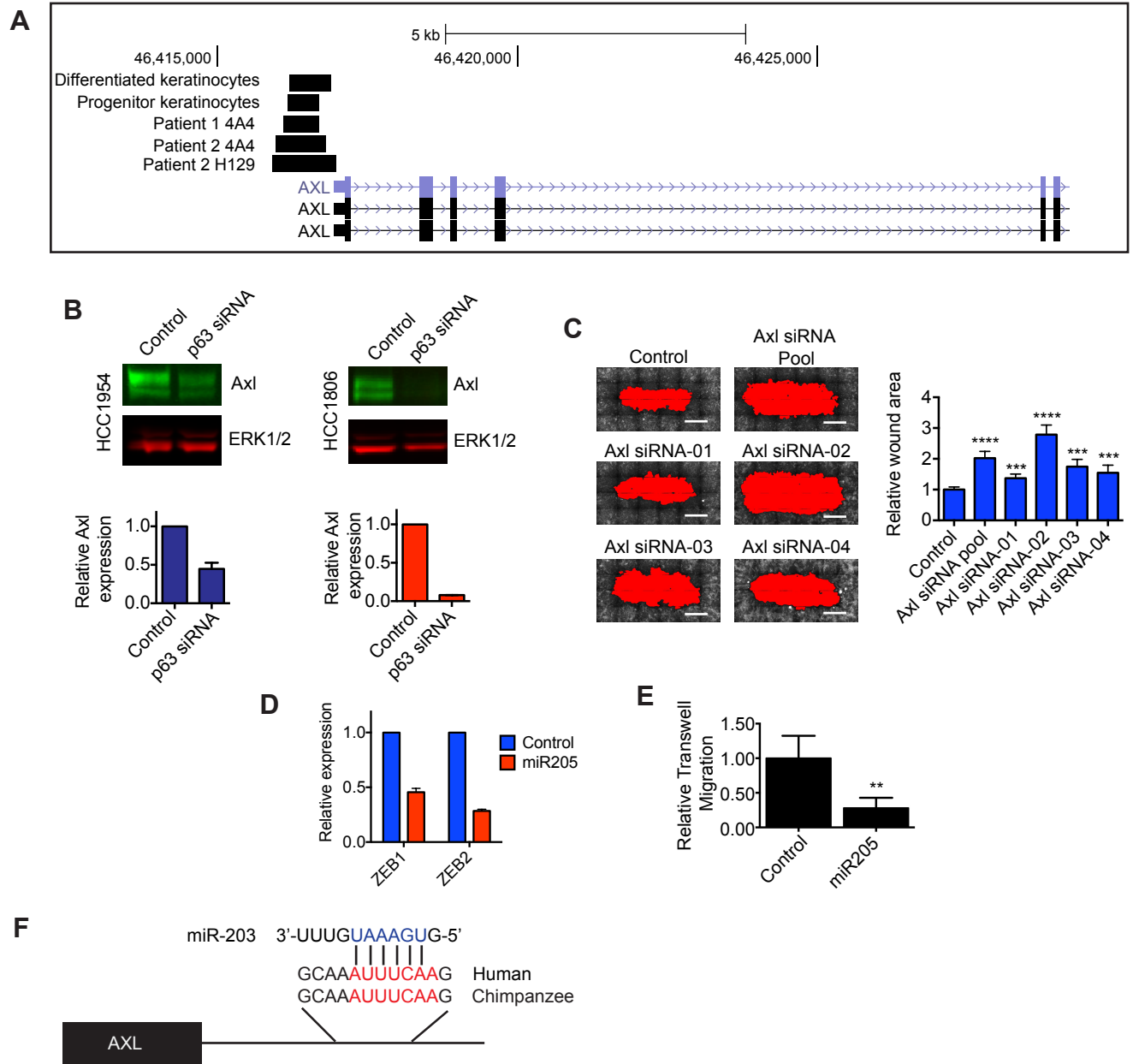
Supplementary Figure S4. Slug expression is regulated by Δ Np63 α . (A) Workflow for identifying candidate genes that are regulated by Δ Np63 α and may be necessary for cell migration. The top Venn diagram shows that 181 genes require Δ Np63 α for expression in MCFDCIS cells and HCC1806 cells (≥ 2 -fold difference in expression between control and p63 siRNA transfected cells, $p < 0.05$). The middle Venn diagram shows that 61 out of the 181 Δ Np63 α dependent genes are expressed at a higher level in motile MCFDCIS and HCC1806 BLBC cells compared to non-motile HCC1428 and MCF7 LBC cells (≥ 2 -fold difference in expression, $p < 0.05$). This suggests that these 61 genes which are regulated by Δ Np63 α may promote BLBC motility. The bottom Venn diagram shows that 11 of the 61 genes regulated by Δ Np63 α are also co-expressed with p63 in breast tumors (Pearson and Spearman's correlation ≥ 0.3). This suggests that Δ Np63 α could potentially regulate the expression of these 11 genes in patient tumors. (B) List of 11 genes that are decreased in expression ≥ 2 fold ($p \leq 0.05$) in MCFDCIS and HCC1806 cells transfected with p63 siRNAs and correlate with p63 expression in breast cancer primary tumors (Pearson and Spearman's correlation ≥ 0.3).

Supplementary Figure S5, Dang et. al.



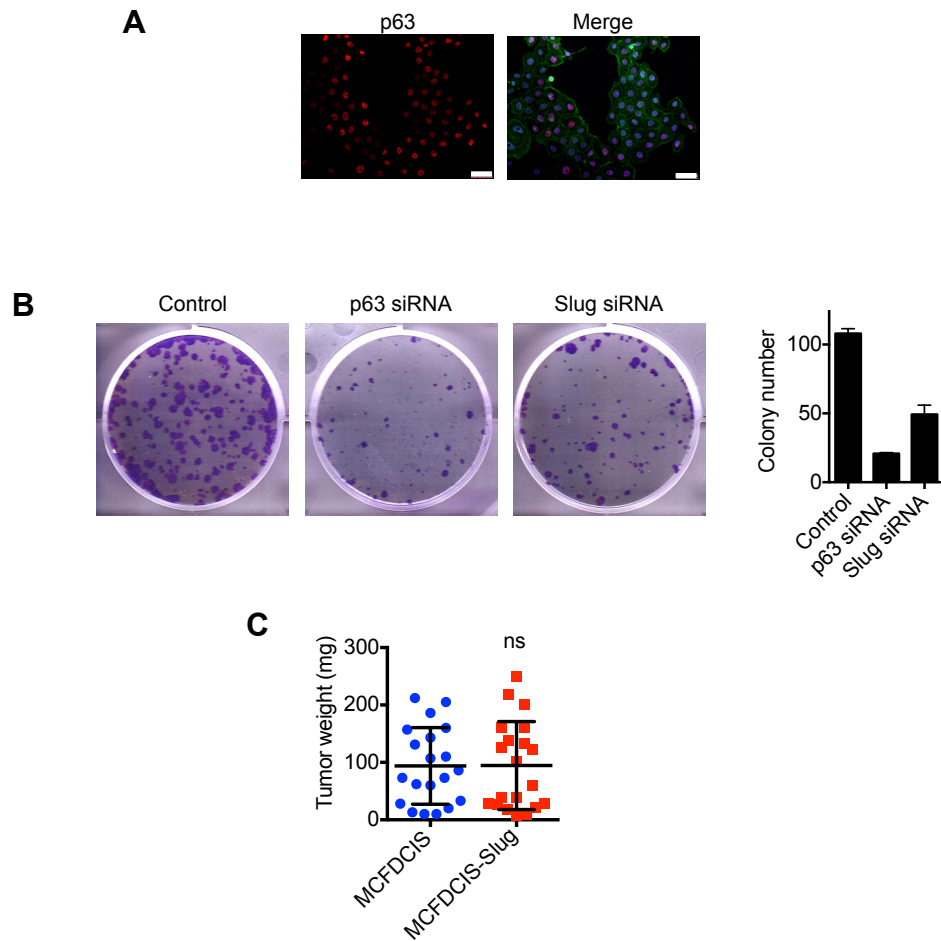
Supplementary Figure S5. Slug is necessary for BLBC motility. (A) Graphs shown quantification of immunoblotting shown in Fig. 3B (n=2, mean + range). (B) Wound healing of MCFDCIS cells transfected with control or Slug siRNAs. Slug siRNA-03 was toxic and was not included in experiments employing a Slug siRNA pool. Scale bars, 1 mm. Graph shows quantification of relative wound area (mean + SD, n= 6 wounds from 2 independent experiments). *p < 0.05, ***, p < 0.001, ****p < 0.0001, Student's t-test. (C) Wound healing of HCC1806 cells transfected with control or Slug siRNAs. Scale bars, 1 mm. Graph shows quantification of relative wound area (mean + SD, n=6 wounds from 2 independent experiments). **p < 0.01, Student's t-test. (D) Subconfluent MCFDCIS cells were transfected as indicated and imaged for 7 h. Scale bars 100 μ m. Graphs show displacement (mean + SD, n= 12 x,y positions over 2 experiments). ****p < 0.0001, Student's t-test.

Supplementary Figure S6, Dang et. al.



Supplementary Figure S6. Axl is required for BLBC motility. (A) UCSC Human Genome Browser view of Axl promoter and gene. The black bars above the Axl gene show peak regions from 5 different samples. (B) Western blots show Axl expression in HCC1954 and HCC1806 cells transfected with the indicated siRNAs. Graphs show relative Axl expression (mean + range, n= 2). (C) Wound healing of MCFDCIS cells transfected with control or Axl siRNAs. Scale bars, 1 mm. Graph shows relative wound area (mean + SD, n=6 wounds from 2 independent experiments). ***, p < 0.001, ****p < 0.0001, Student's t-test. (D) Graph shows the relative expression of ZEB1 and ZEB2 in 578T cells transfected with miR205 as determined by q-PCR (mean + range, n=2 experiments performed in triplicate). (E) Graph shows relative transwell migration of MDA-MB-231 cells transfected with a control or miR205 mimic (mean + SD, n=3). **p < 0.01, unpaired Student's t-test. (F) Graphic showing the predicted miR203a target sequence in the 3' UTR of the Axl gene in the indicated species using Targetscan.

Supplementary Figure S7, Dang et. al.



Supplementary Figure S7. Δ Np63 α and Slug are required for cell growth. (A) MCFDCIS cells in monolayer culture immunostained with anti-p63 antibody (red) and counterstained with phalloidin (green) and Hoechst (blue). Scale bars, 50 μ m. (B) Colony forming assay showing the growth of MCFDCIS cells transfected with the indicated siRNAs. Graph shows the number of colonies containing \geq 50 cells (mean + range n=2, in duplicate). (C) Graph shows the weights of MCFDCIS and MCFDCIS-Slug tumors (n=20 mice, for both groups). There was no significant difference in tumor weights, unpaired Student's t-test.

Supplementary Legends

Supplementary Table S1. Wound healing activity scores, z-scores and relative fluorescence values for all 879 miRNA mimics.

Supplementary Table S2. The wound healing z-scores and relative fluorescence values for the 574 miRNA mimics that had a relative fluorescence of ≥ -50 .

Supplementary Table S3. The wound healing z-scores for the re-tested 132 miRNAs.

Supplementary Table S4. MiRNAs that are differentially expressed in MCFDCIS compared to HCC1428 cells. ≥ 2 fold difference in expression, $p \leq 0.05$.

Supplementary Table S5. The wound healing z-scores and relative fluorescence values of miRNAs differentially expressed between MCFDCIS and HCC1428 cells. MiRNAs from Supplementary Table S4 that were tested in the wounding screen and had a relative fluorescence of ≥ -40 are shown.

Supplementary Table S6. Genes co-expressed with miR205HG in breast cancer patient primary tumors. Pearson correlation and Spearman's correlation ≥ 0.3 .

Supplementary Table S7. Genes that are differentially expressed in MCFDCIS cells or HCC1806 cells transfected with p63 siRNAs. ≥ 2 fold difference in expression, $p \leq 0.05$.

Supplementary Table S8. Genes that are differentially expressed in MCFDCIS and HCC1806 cells (motile BLBC cells) compared to HCC1428 and MCF7 cells (non-motile LBC cells). ≥ 2 fold difference in expression, $p \leq 0.05$.

Supplementary Table S9. Genes that are regulated by Δ Np63 α and differentially expressed between motile BLBC cells (MCFDCIS and HCC1806) and non-motile cells LBC cells (HCC1428 and MCF7).

Supplementary Table S10. Genes co-expressed with p63 in breast cancer patient primary tumors.
Pearson and Spearman's correlation ≥ 0.3 .

Supplementary Table S11. List of antibodies used.

Supplementary Table S12. List of siRNA sequences used.

Supplementary Methods

Cell culture. Cells were cultured at 5% CO₂, humidified, and at 37 ° C. MCFDCIS cells were cultured in DME-F12, 5% horse serum, 20 ng/ml EGF, 0.5 µg/ml hydrocortisone, 100 ng/ml cholera toxin, 10 µg/ml insulin and 1X pen/strep. SUM149 cells were cultured in Mammary Epithelial Growth Medium (MEGM, Lonza). All other cell lines were cultured in 10% FBS RPMI. ΔNp63α (Addgene, 26979), (1), was cloned into a PLX302 (Addgene, 25896), (2), using the Gateway cloning system (Invitrogen) according to manufacturers' protocol. Retroviral plasmids containing Slug (Addgene, 25696), and Axl (Addgene, 20428), (3), were used. Virus was produced and cells were infected to generate stable cell lines as described (4).

Western blots. Cells were lysed as described (4). Lysates were immunoblotted with the antibodies described in Supplemental Table S11.

Transfections. Cells were reverse transfected in glass-bottom 96-well plates (BD Biosciences) with RNAiMax (Invitrogen). See Supplemental Table S12 for a list of siRNAs and miRNAs used. Unless otherwise indicated, all transfections were performed as follows: Control siRNA- 50 nM "Non-targeting" siRNA pool (Dharmacon); p63 siRNA- 50 nM (pool #1, #2 and #3, Sigma); Slug siRNA- 5 nM (pool #1, 2 and 4, Dharmacon); Axl siRNA, 50 nM (pool #1, #2, #3, #4, Dharmacon); Control miRNA (miR545) 10 nM miR203- 10 nM (Dharmacon) and miR205- 10 nM (Dharmacon).

Wounding Assay. Wounds were generated with 96-pin wounding tool (AFIX96FP6, V&P Scientific) containing 1.68 mm diameter pins (FP6-WP) and a monolayer wounding library copier that introduces a wound length of 4.5 mm (VP 381NW 4.5, V&P Scientific). Immediately after wounding wells were washed twice with media to remove debris. Twenty-four hours after wounding, cells were fixed in 2% formalin and stained with phalloidin-546 and Hoechst. Wounds were imaged on a BD

Pathway 855 microscope with a 10x objective (Olympus, UPlanSApo 10x/0.40, ∞ /0.17/FN26.5). Images were acquired as 4x5 or 6x4 montages.

Spontaneous motility assay. Cells expressing H2B:GFP were reverse transfected and grown for 72 h in 96-well glass bottom plates. Time-lapse imaging was performed for 7 h total with images acquired at 30 min intervals. Tracking of cell movement to measure change in displacement and speed was performed with Imaris software as described (4).

Transwell migration assay. MDAMB231-H2B:GFP cells were transfected for 24 h and plated at a density of 20,000 cells/ transwell filter (BD Falcon Cell Culture Inserts, 353097) in 1% FBS/RPMI media. Cells were then allowed to migrate towards a reservoir of 10% FBS/RPMI for 6 h. Non-migrating cells were removed from the upper side of the transwell filter with a cotton swab and migrated cells on the bottom side of the transwell filter were counted using an inverted fluorescence microscope.

Immunofluorescence for wounding assays. Media was removed from the 96-well plates and rinsed with 1X PBS. Cells were fixed with 2% formalin for 20 minutes and permeabilized with 0.05% Triton X-100 for 10 minutes. Cells were blocked with 10% goat serum diluted in IF buffer (0.1% BSA, 0.2% Triton X-100, 0.05% Tween-20 in PBS) for 1 h and stained with 1:250 Phalloidin-546 (Life Technologies, A22283) and 1:2000 Hoechst (Life Technologies, H1399) for 1 hour. Plates were then washed 3 times with IF Buffer, rinsed with 1X PBS, and stored in 1X PBS at 4° C until imaged.

Immunofluorescence for paraffin embedded tumor sections. Tumor sections were deparaffinized with three 10 minute washes of xylene, re-hydrated with two 3 minute washes each of 100%, 95%, 70%, and 50% of EtOH diluted with water, one 3 minute wash of PBS and antigen retrieval with 1X boiling sodium citrate, pH 6.5 for 20 minutes. The sections were then washed once with PBS

and then blocked for 30 minutes in 20% AquaBlock (Fisher, NC9336595) diluted in 1X TBS. Primary antibodies were diluted in 5%BSA/TBS and applied to the sections for overnight at 4° C. Sections were washed with PBST (0.5% Tween-20 in PBS) for three times, 5 minutes each. Secondary antibodies were applied at 1:500 dilution in 5%BSA/TBS for 1 h in the dark. Sections were washed with PBST (0.5% Tween-20 in PBS) for three times, 5 minutes each. Slides were mounted with Prolong Gold (Life Technologies, P36930) and incubated in the dark overnight.

Time-lapse imaging. Imaging was performed using a Perkin Elmer Ultraview ERS spinning disk confocal microscope enclosed in a 37°C chamber supplemented with humidified CO₂ (Solent) and a CCD camera (Orca AG; Hamamatsu). Images were acquired for at least 5 x.y points per condition for 7 h at 30 min intervals in each experiment with a 10x (Zeiss) objective using Volocity software (Perkin Elmer). Cell displacement and speed were determined with Imaris software (Bitplane) as described (4).

Quantitative real-time PCR. Total RNA was isolated using RNAeasy purification columns (Qiagen) and converted to cDNA using the iScript cDNA Synthesis Kit (Bio-Rad). Applied Biosystems TaqMan Gene Expression Assays were performed with 20 ng of cDNA was amplified with Applied Biosystems 2X TaqMan using an Applied Biosystems 7500 Real-Time PCR System. GAPDH and specific transcript levels for each transfection condition were measured in triplicate. The $\Delta\Delta CT$ method was applied to quantify relative gene expression (5). MiR203a (000507), miR205 (00509), p63 (Hs_00978343_m1), Slug (Hs_00950344_m1), Axl (Hs_01064444_m1) and GAPDG (H2_02758991_g1) primers (Life Technologies) were used.

Gene and miRNA expression profiling. The mRNA expression was determined using Human HT-12 v4 Expression BeadChips (Illumina Inc.). MiRNA expression was determined using Exiqon 7th generation arrays (#208502). Data was processed with a model-based background correction approach

(6), quantile-quantile normalization and log₂ transformation. Heatmaps showing the relative expression of genes were generated with GenePattern software using the HeatMapImage module (7). The mRNA and miRNA expression data are available at the GEO (GSE58643, GSE62569).

Xenografts. Age-matched female NOD/SCID mice were used for all in vivo experiments. When possible, littermates were housed together. NOD/SCID mice were obtained from The Jackson Laboratory (Bar Harbor, ME), and bred and maintained under specific pathogen-free conditions in a barrier facility at the University of Texas Southwestern Medical Center (Dallas, TX). All experiments were performed in compliance with the relevant laws and institutional guidelines of the University of Texas Southwestern Medical Center. 50,000 MCFDCIS cells, 50,000 MCFDCIS cells combined with 200,000 mammary fibroblasts or 50,000 MCFDCIS-Slug cells were injected in the fourth mammary fat pad of 6-8 weeks NOD/SCID female mice as described (4). Three weeks after injection, mice were sacrificed and the tumors were removed for embedding in paraffin.

ChIP RT-PCR. ChIP was performed as described (8) with the exception that 1% formalin was used for cross-linking. Anti-p63 (Santa Cruz, H-129) and normal rabbit IgG (Santa Cruz, 2027) were used for immunoprecipitation. Primers for Axl were forward: -0.41 kb, 5' ATTTGGTGTCCCATTTAGGC 3'; reverse: - 0.2 kb 5' TCGATTCCTGGAGAAACCTC 3'. The following primers were used for non-binding (12th exon of Axl): 5'-CCTGGCCTGGATCTAAAGG-3' and 5'-GGGTCTGTGGTTCTGACATTC-3'. % Input was determined as $(2^{-(\text{Average Ct for Input} - \text{Ct of sample})}) \times (\% \text{ Input used in qPCR}) \times 100$. For ChIP RT-PCR, BioRAD iTaq Universal SYBR Green Master Mix was used. In a 20 ul reaction, 2 ul of chromatin, 10 ul of SYBR Green, 1 uM of primers and up to 20 ul of water. Temperatures and times for RT-PCR followed manufacturer's protocol for ABI 7500 instrument.

Colony formation assay. Cells were transfected with siRNAs for 72 hours before re-plating at a density of 300 cells per well in a 6-well plate. Colonies grew 7 days and were fixed with formalin and stained with Giemsa (Sigma Aldrich).

Wounding screen. Master plates were aliquoted into three replicate plates at a final concentration of 50 nM miRNA mimic with a robotic replica plating system. A Titertek multi-drop was used to add RNAiMax (Invitrogen) and 10,000 MCFDCIS cells to each well in a reverse transfection format. Reference plates containing mock transfected cells (no miRNA) were interspersed within the plating procedure to control for plating variation during data analysis. Wounds were generated with 96-pin wounding tool (described in the “Wounding Assay section”). Twenty-four hours after wounding, cells were fixed in formalin and stained with phalloidin-AlexaFluor-546 and Hoechst with a Titertek multi-drop system. For wound closure analysis, a 4x5 montage of images of each well acquired using a BD Pathway 855 microscope equipped with a 10x objective (Olympus, UPlanSApo 10x/0.40, ∞ /0.17/FN26.5). To determine the relative number of cells per well, after wounding images were acquired, the Hoechst signal in each well was determined with a Pherastar plate reader. A custom designed analysis protocol was generated using Pipeline Pilot software, which used a threshold of pixel signal intensity to determine the amount of empty space in each well not occupied by cells. The amount of empty space in the well was inversely proportional to the extent of wound closure. Wounding activities were normalized to internal controls and z-scores were calculated ($z \text{ score} = (\text{miRNA Activity Score} - \text{Mean Activity score of mock transfected cells}) / (\text{Standard deviation of mock transfected cells})$). Fluorescence values were normalized to internal controls.

Supplementary References

1. Chatterjee A, Upadhyay S, Chang X, Nagpal JK, Trink B, Sidransky D. U-box-type ubiquitin E4 ligase, UFD2a attenuates cisplatin mediated degradation of DeltaNp63alpha. *Cell Cycle* 2008;7:1231-7.
2. Yang X, Boehm JS, Yang X, Salehi-Ashtiani K, Hao T, Shen Y, et al. A public genome-scale lentiviral expression library of human ORFs. *Nat Methods* 2011;8:659-61.
3. Boehm JS, Zhao JJ, Yao J, Kim SY, Firestein R, Dunn IF, et al. Integrative genomic approaches identify IKBKE as a breast cancer oncogene. *Cell* 2007;129:1065-79.
4. Dang TT, Precht AM, Pearson GW. Breast cancer subtype-specific interactions with the microenvironment dictate mechanisms of invasion. *Cancer Res* 2011;71:6857-66.
5. Bookout AL, Cummins CL, Mangelsdorf DJ, Pesola JM, Kramer MF. High-throughput real-time quantitative reverse transcription PCR. *Current protocols in molecular biology* / edited by Frederick M Ausubel [et al] 2006;Chapter 15:Unit 15 8.
6. Xie Y, Wang X, Story M. Statistical methods of background correction for Illumina BeadArray data. *Bioinformatics* 2009;25:751-7.
7. Reich M, Liefeld T, Gould J, Lerner J, Tamayo P, Mesirov JP. GenePattern 2.0. *Nat Genet* 2006;38:500-1.
8. Ramsey MR, He L, Forster N, Ory B, Ellisen LW. Physical association of HDAC1 and HDAC2 with p63 mediates transcriptional repression and tumor maintenance in squamous cell carcinoma. *Cancer research* 2011;71:4373-9.